Structural and Electrical Properties of Lead-Free $Ba(Sn,Ti)O_3$–$(Na_{0.5}K_{0.5})NbO_3$ Ceramics

Chun-Huy Wang* and Jun-Jie Wang

Department of Electronic Engineering, Nan-Jeon Institute of Technology, Tainan, Taiwan 737, R.O.C.

Received September 9, 2008; accepted January 4, 2009; published online April 20, 2009

$(Na_{0.5}K_{0.5})NbO_3$ with $Ba(Sn_xTi_{1-x})O_3$ with $x < 0.1$ has been prepared by the conventional mixed oxide process. X-ray diffraction analysis revealed that, during sintering, all the $Ba(Sn_xTi_{1-x})O_3$ diffuses into the lattice of $(Na_{0.5}K_{0.5})NbO_3$ to form a solid solution and the orthorhombic phase with a perovskite structure. The highest planar coupling factor of $0.98(Na_{0.5}K_{0.5})NbO_3$–$0.02Ba(Sn_{0.02}Ti_{0.98})O_3$ ceramics is 0.31 after sintering at 1100 °C for 3 h. The samples with a low content of $Ba(Sn_{0.06}Ti_{0.94})O_3$ exhibit relatively good physical and electrical properties. For $0.98(Na_{0.5}K_{0.5})NbO_3$–$0.02Ba(Sn_{0.06}Ti_{0.94})O_3$ ceramics, the electromechanical coupling coefficients of the planar mode k_p and the thickness mode k_t reach 0.18 and 0.46, respectively, after sintering at 1100 °C for 3 h. The ratio of the thickness coupling coefficient to the planar coupling coefficient is 2.56. With suitable $Ba(Sn_xTi_{1-x})O_3$ concentration and sintering conditions, a dense microstructure and good electrical properties are obtained. Our results show that $(Na_{0.5}K_{0.5})NbO_3$–$Ba(Sn_{0.06}Ti_{0.94})O_3$ solid solution ceramics are promising lead-free ceramics for high-frequency electromechanical transducer applications.
© 2009 The Japan Society of Applied Physics

DOI: 10.1143/JJAP.48.041403

1. Introduction

Ever since the discovery of the piezoelectric effect, piezoelectric materials have been rapidly developed and widely used. At present, the most widely-used piezoelectric materials are $Pb(Zr,Ti)O_3$ (PZT)-based ceramics because of their superior piezoelectric properties. However, the high volatility and toxicity of PbO during firing can contaminate the environment and damage human health. With the rise of environmental consciousness, therefore, it is the current tendency to develop excellent lead-free materials to replace Pb-based piezoelectric ceramics. Lead-free piezoelectric materials such as sodium potassium niobate-based oxides, bismuth layer-structure oxides, and tungsten bronze oxides have been studied to replace PZT-based ceramics. Among them, $(Na_{0.5}K_{0.5})NbO_3$ (NKN) ceramics are considered good candidates for lead-free piezoelectric ceramics because of their strong piezoelectricity and ferroelectricity.

The hot-pressed NKN ceramics (~99% of theoretical density) have been reported to possess a large piezoelectric longitudinal response ($d_{33} \sim 160$ pC/N), a high planar coupling coefficient ($k_p \sim 45\%$), and a high phase transition temperature ($T_c = 420$ °C).[1] NKN ceramics sintered by ordinary sintering show relatively lower values ($k_p = 25\%$) due to difficulty in the processing of dense ceramics by ordinary sintering.[2] This issue has received significant attention and has been thoroughly investigated.[3–5] Nevertheless, dense NKN ceramics are difficult to obtain since their phase stability is limited to 1140 °C, which is close to the melting point.[6] Many researchers used hot pressing or spark plasma sintering (SPS) techniques to yield better quality ceramics.[7] Recently, an efficient solution to improve these problems has been realized by using some additives in NKN ceramics, such as ZnO,[8] $BaTiO_3$,[9] $LiNbO_3$,[10] $LiTaO_3$,[11] $SrTiO_3$,[12,13] and $CaTiO_3$.[14,15] A comparison of the properties of $(Na_{0.5}K_{0.5})NbO_3$ ceramics based on the previous reports of various groups is shown in Table I. The addition of some perovskite compounds to form solid solutions with NKN or synthesis by spark plasma sintering (SPS) has been carried out to obtain lead-free materials suitable for industrial applications. Recent electromechanical studies[16,17] have demonstrated that $Ba(Sn_xTi_{1-x})O_3$ (BST) is basically suitable as an environmental-friendly material for electromechanical sensor and actuator applications.

The aim of this study is not only to investigate the physical and electrical properties of the $(Na_{0.5}K_{0.5})NbO_3$–$Ba(Sn_xTi_{1-x})O_3$ system by the conventional mixed oxide method, but also to produce a large anisotropy in the electromechanical coupling factor k_t/k_p for high-frequency electromechanical transducer applications. The effects of sintering time on the structural and electrical properties of $0.98(Na_{0.5}K_{0.5})NbO_3$–$0.02Ba(Sn_{0.06}Ti_{0.94})O_3$ ceramics are also discussed.

2. Experimental Procedure

The $0.98(Na_{0.5}K_{0.5})NbO_3$–$0.02Ba(Sn_xTi_{1-x})O_3$ ceramics (abbreviated NKN–BST) were prepared by a solid-state reaction method. The starting materials were K_2CO_3, Na_2CO_3, $BaCO_3$, Nb_2O_5, TiO_2, and SnO_2 with purities of at least 99.5% and weighted according to the stoichiometric composition ($x = 0$, 0.02, 0.04, 0.06, and 0.08). The powders were calcined at 950 °C for 10 h. The calcined powders were pressed (CIP) at 180 MPa into pellets 15 mm in diameter. The disc samples were sintered in alumina crucibles at 1100 °C for 3–7 h in air. To measure the relevant piezoelectric properties, the ceramic samples were polarized in silicone oil at 100 °C at 4 kV/mm for 30 min. An X-ray diffractometer (Seimens D5000) using Cu Kα radiation was used to evaluate the crystal structure of the sintered ceramics. The room temperature dielectric constant was measured by an impedance analyzer (Agilent 4284A) at about 1 kHz. The piezoelectric properties were measured by a resonance-antiresonance method based on IEEE standards using an impedance/gain-phase analyzer (Agilent 4194). The samples for observation of the microstructure were polished and thermaly etched. The microstructures were observed using a scanning electron microscope (SEM). The mean grain size was calculated by the line intercept method.[18] The density was measured by Archimedes' method.

*E-mail address: wch70982@ms41.hinet.net

 © 2009 The Japan Society of Applied Physics

Table I. Comparison of properties of $(Na_{0.5}K_{0.5})NbO_3$ ceramics based on previous reports of various groups.

Composition	Measured density (g/cm^3)	Relative density (%)	K_0	k_p	k_t	k_t/k_p	Ref.
NKN	4.34	96.4	—	0.295	0.41	1.39	9
NKN–ZnO	4.26	94.5	500	0.4	—	—	8
$0.98NKN–0.02BaTiO_3$	4.44	98.4	—	0.29	0.38	1.31	9
$0.995NKN–0.005SrTiO_3$	4.44	98.4	412	0.325	0.438	1.35	13
$0.94NKN–0.06LiNbO_3$	4.35	96.5	—	0.42	0.48	1.14	10
$0.94NKN–0.06LiTaO_3$	—	—	570	0.36	—	—	11
$0.995NKN–0.005CaTiO_3$	4.4	97.6	553	0.42	0.38	1.1	14
$0.98NKN–0.02Ba(Sn_{0.06}Ti_{0.94})O_3$	4.32	96	418	0.24	0.49	2.04	This study

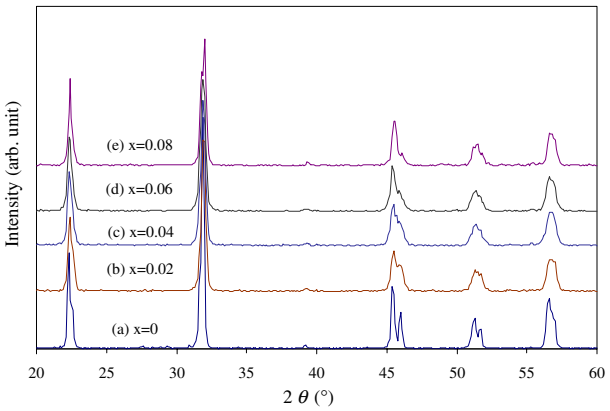

Fig. 1. (Color online) XRD patterns of $0.98(Na_{0.5}K_{0.5})NbO_3$–$0.02Ba(Sn_xTi_{1-x})O_3$ ceramics system for differenr x compositions: (a) 0, (b) 0.02, (c) 0.04, (d) 0.06, and (e) 0.08.

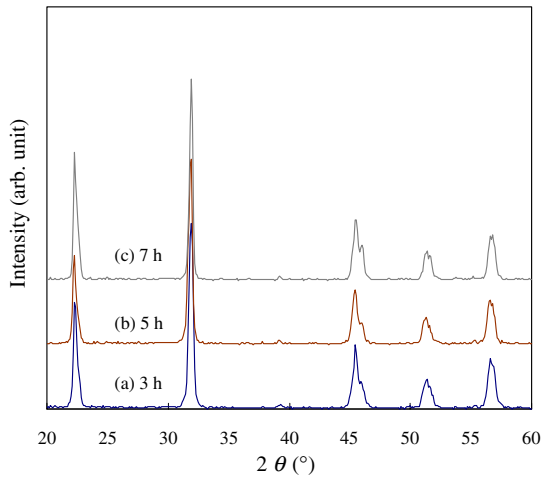

Fig. 2. (Color online) XRD patterns of $0.98(Na_{0.5}K_{0.5})NbO_3$–$0.02Ba(Sn_{0.06}Ti_{0.94})O_3$ ceramics system sintered at 1100 °C for different times: (a) 3, (b) 5, and (c) 7 h.

3. Results and Discussion

In this system, none of the samples showed deliquescence when exposed under water for a long period, indicating no existence of the unstable second phase. Figure 1 shows the X-ray diffraction (XRD) patterns of $0.98(Na_{0.5}K_{0.5})NbO_3$–$0.02Ba(Sn_xTi_{1-x})O_3$ ceramics for $x = 0$, 0.02, 0.04, 0.06, and 0.08. All the compositions were sintered in air at 1100 °C for 3 h. The orthorhombic symmetry of 0.98NKN–0.02BST ceramics at room temperature is characterized in the XRD patterns in the 2θ range of 44–48°. The XRD analysis of sintered samples shows that 0.98NKN–0.02BST has a single phase with a perovskite structure and forms a solid solution. In addition, it is obvious that the diffraction peaks shift toward a higher angle with increasing BST content, since it is expected that Ba^{+2} (1.61 Å ionic radius) could substitute for Na^{+1} (1.39 Å) and K^{+1} (1.64 Å), while Ti^{+4} (0.61 Å) and Sn^{+4} (0.69 Å) could substitute for Nb^{+5} (0.64 Å). Figure 2 shows the XRD patterns of the $0.98(Na_{0.5}K_{0.5})NbO_3$–$0.02Ba(Sn_{0.06}Ti_{0.94})O_3$ ceramics system sintered at 1100 °C for different sintering time (3, 5, and 7 h). Only an orthorhombic phase with a perovskite structure was observed. The BST appears to have diffused into the NKN lattice to form a solid solution in which Ba occupies the (Na,K) lattice and (Ti,Sn) enters the Nb sites of NKN.

Figure 3 shows the microstructure of the $0.98(Na_{0.5}K_{0.5})NbO_3$–$0.02Ba(Sn_{0.06}Ti_{0.94})O_3$ ceramics sintered at 1100 °C for different times: (a) 3, (b) 5, and (c) 7 h. It can be seen in Fig. 3(a) that the $0.98(Na_{0.5}K_{0.5})NbO_3$–$0.02Ba(Sn_{0.06}Ti_{0.94})O_3$ ceramics consist of small grains with a loose structure and a high porosity. However, the $0.98(Na_{0.5}K_{0.5})NbO_3$–$0.02Ba(Sn_xTi_{1-x})O_3$ ceramics sintered for 5 h are more dense, with low porosity, and exhibit greater homogeneity and a grain size of ~1.8 µm, as shown in Fig. 3(b). As shown in Fig. 3(c), a longer sintering time may cause excessive NKN loss and a resultant variation in composition, which leads to an inhomogeneous microstructure. These conditions may increase the porosity because of a greater rate of evaporation of NKN compared with its recondensation.

Figures 4 and 5 show the physical and electrical properties of $0.98(Na_{0.5}K_{0.5})NbO_3$–$0.02Ba(Sn_xTi_{1-x})O_3$ ($x = 0$, 0.02, 0.04, 0.06, and 0.08) sintered at 1100 °C for 3 h. The measured density and dielectric constant of $0.98(Na_{0.5}K_{0.5})NbO_3$–$0.02Ba(Sn_xTi_{1-x})O_3$ ceramics are shown as functions of Sn composition in Fig. 4. The measured density of the sintered samples is 90–96% of the theoretical density. The measured density and dielectric constant increase with an increase in Sn content. The planar coupling factor (k_p) and thickness coupling factor (k_t) of $0.98(Na_{0.5}K_{0.5})NbO_3$–$0.02Ba(Sn_xTi_{1-x})O_3$ ceramics are shown as functions of Sn composition in Fig. 5. The electromechanical coupling factor is related to different Sn content. The electromechanical coupling factor has been used extensively as a measure of the piezoelectric response of PZT-based ceramics. It was found that the electromechanical coupling factor depended

© 2009 The Japan Society of Applied Physics

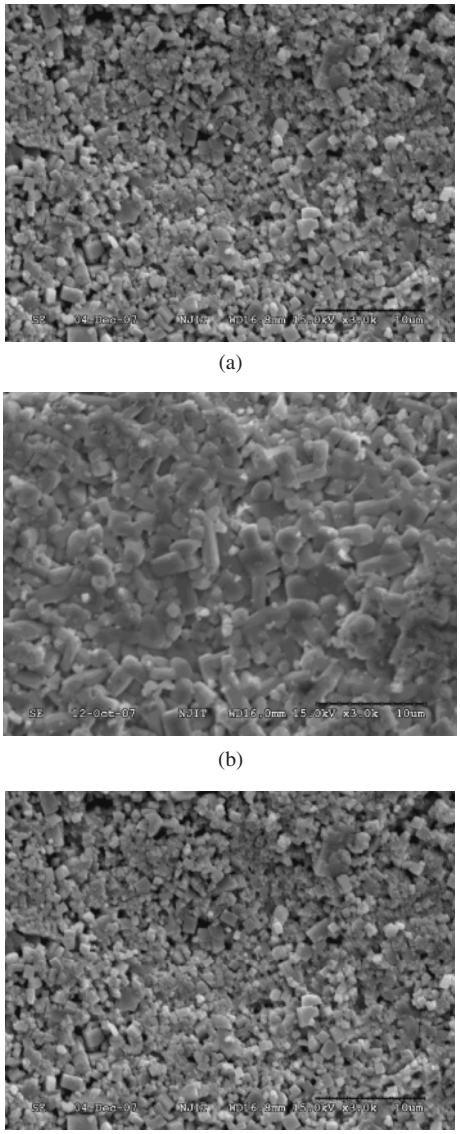

(a)

(b)

(c)

Fig. 3. SEM images of $0.98(Na_{0.5}K_{0.5})NbO_3$–$0.02Ba(Sn_{0.06}Ti_{0.94})O_3$ ceramics sintered at 1100 °C for different times: (a) 3, (b) 5, and (c) 7 h.

on the material parameters[19] such as grain size, porosity, and chemical composition. Usually, the piezoelectric activity increases with the value of the electromechanical coupling factor in radial mode k_p and in thickness mode k_t. The equations for calculating electromechanical coupling factors k_p and k_t are

$$\frac{1}{k_p^2} = 0.395\frac{f_r}{f_a - f_r} + 0.574,$$

$$\frac{1}{k_t^2} = 0.81\frac{f_r}{f_a - f_r} + 0.405,$$

where f_r is a resonant frequency and f_a is an antiresonant frequency. The highest planar coupling factor ($k_p = 0.31$) of $0.98(Na_{0.5}K_{0.5})NbO_3$–$0.02Ba(Sn_xTi_{1-x})O_3$ ceramics is found at $x = 0.02$. For $0.02Ba(Sn_{0.06}Ti_{0.94})O_3$–$0.98(Na_{0.5}K_{0.5})NbO_3$ ceramics, the electromechanical coupling coefficients of the planar mode k_p and the thickness mode k_t reach 0.18 and 0.46, respectively, after sintering at 1100 °C for 3 h. The ratio of the thickness coupling coefficient to the planar coupling coefficient is 2.56, as shown in Table II.

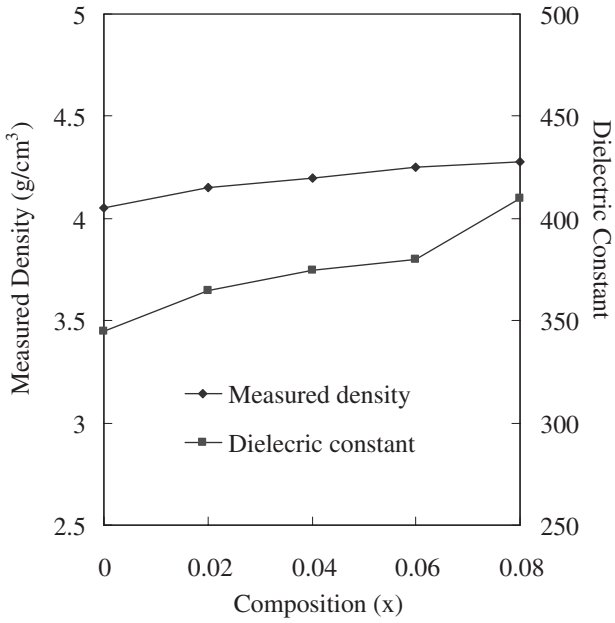

Fig. 4. Measured density and dielectric constant of $0.98(Na_{0.5}K_{0.5})NbO_3$–$0.02Ba(Sn_xTi_{1-x})O_3$ ceramics sintered at 1100 °C for 3 h with different compositions.

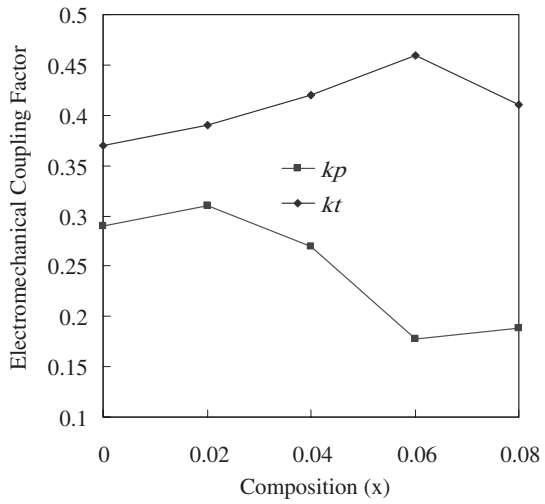

Fig. 5. Planar coupling factor k_p and thickness coupling factor k_t of $0.98(Na_{0.5}K_{0.5})NbO_3$–$0.02Ba(Sn_xTi_{1-x})O_3$ ceramics sintered at 1100 °C for 3 h with different compositions.

Table II. Physical and electrical properties of $0.98(Na_{0.5}K_{0.5})NbO_3$–$0.02Ba(Sn_xTi_{1-x})O_3$ ceramics sintered at 1100 °C for different compositions and sintering times.

Composition x	Sintering time (h)	Relative density (%)	Grain size (μm)	k_p	k_t	k_t/k_p	K_0	K_{33}^T
0.08	3	95.1	1.1	0.19	0.41	2.18	410	385
0.06	7	92.9	2.1	0.22	0.42	1.99	401	350
0.06	5	96	1.8	0.24	0.49	2.04	418	375
0.06	3	94.4	0.9	0.18	0.46	2.56	380	360
0.04	3	93.3	0.8	0.27	0.42	1.55	375	345
0.02	3	92.2	0.7	0.31	0.39	1.44	365	331
0	3	90	0.5	0.29	0.37	1.27	345	324

© 2009 The Japan Society of Applied Physics

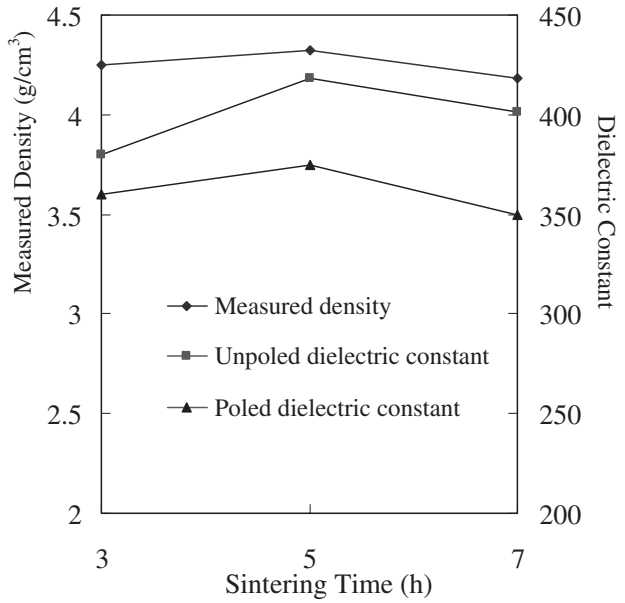

Fig. 6. Measured density and dielectric constant of $0.98(Na_{0.5}K_{0.5})NbO_3$–$0.02Ba(Sn_{0.06}Ti_{0.94})O_3$ ceramics sintered at 1100 °C for different times.

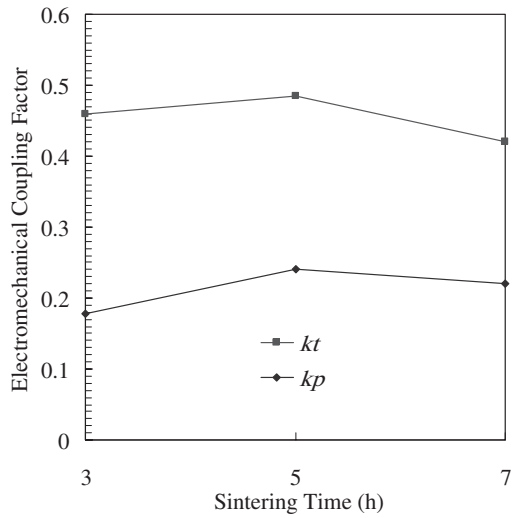

Fig. 7. Planar coupling factor k_p and thickness coupling factor k_t of $0.98(Na_{0.5}K_{0.5})NbO_3$–$0.02Ba(Sn_{0.06}Ti_{0.94})O_3$ ceramics sintered at 1100 °C for different times.

Figures 6 and 7 show the physical and electrical properties of $0.02Ba(Sn_{0.06}Ti_{0.94})O_3$–$0.98(Na_{0.5}K_{0.5})NbO_3$ ceramics sintered at 1100 °C for different sintering times (3, 5, and 7 h). The measured density and dielectric constant of $0.02Ba(Sn_{0.06}Ti_{0.94})O_3$–$0.98(Na_{0.5}K_{0.5})NbO_3$ ceramics sintered at 1100 °C are shown as functions of sintering time in Fig. 6. The measured density and dielectric constant increase with increasing sintering time up to 5 h, then decrease at 7 h. The dielectric constants K_0 (before polarization) and K_{33}^{T} (after polarization) of $0.98(Na_{0.5}K_{0.5})NbO_3$–$0.02Ba(Ti_{0.94}Sn_{0.06})O_3$ ceramics are shown as functions of sintering time in Fig. 6. In piezoelectric ceramics, the properties depend on the composition and crystal structure; the dielectric constant may be increased or decreased through poling. Moreover, the variations of the dielectric constant through poling also rely on domain alignment. In an orthorhombic phase, the dielectric constant decreases after poling, and the net decrease is due to the 90° domain reorientation dominating the effect of the removal of compression.[20–22] In the orthorhombic phase, K_{33}^{T} decreases in comparison to K_0 as a result of the dielectric anisotropy.

The planar coupling factor (k_p) and thickness coupling factor (k_t) of $0.02Ba(Sn_{0.06}Ti_{0.94})O_3$–$0.98(Na_{0.5}K_{0.5})NbO_3$ ceramics are shown as functions of sintering time in Fig. 7. The planar coupling factor (k_p) and thickness coupling factor (k_t) increase with increasing sintering time up to 5 h, then decrease at 7 h. For $0.98(Na_{0.5}Bi_{0.5})TiO_3$–$0.02Ba(Sn_{0.06}Ti_{0.94})O_3$ ceramics, the electromechanical coupling coefficients of the planar mode k_p and the thickness mode k_t reach 0.24 and 0.485, respectively, after sintering at 1100 °C for 5 h. The ratio of the thickness coupling coefficient to the planar coupling coefficient is 2.02, as shown in Table II.

Table II shows the physical and electrical properties of $0.98(Na_{0.5}K_{0.5})NbO_3$–$0.02Ba(Sn_xTi_{1-x})O_3$ ceramics sintered at 1100 °C for different compositions and sintering times. The relative density is the ratio of the measured density to the theoretical density. The relative density and the grain size of $0.98(Na_{0.5}K_{0.5})NbO_3$–$0.02Ba(Sn_xTi_{1-x})O_3$ ceramics increased with increasing Sn content after sintering at 1100 °C for 3 h. The relative density and the grain size of $0.02Ba(Sn_{0.06}Ti_{0.94})O_3$–$0.98(Na_{0.5}K_{0.5})NbO_3$ ceramics are 94.4% and 0.9 µm, respectively, after 3 h of sintering at 1100 °C. By prolonging the sintering time to 5 h, the relative density was raised to 96% and the grain size was increased to 1.8 µm. In this system, the properties have better values for 5 h of sintering at 1100 °C. By prolonging the sintering time to 7 h, the relative density was decreased to 92.9% and the grain size was increased to 2.1 µm. From the SEM images as shown in Fig. 3(c), a longer sintering time may cause excessive NKN loss and a resultant variation in composition, which leads to an inhomogeneous microstructure. This may increase the porosity, because of a greater rate of evaporation of NKN compared with its recondensation. With increasing porosity of $0.02Ba(Sn_{0.06}Ti_{0.94})O_3$–$0.98(Na_{0.5}K_{0.5})NbO_3$ ceramics, the piezoelectric and dielectric properties diminish gradually. The physical and electrical properties have better values for 5 h of sintering at 1100 °C. A comparison of the properties of $(Na_{0.5}K_{0.5})NbO_3$ ceramics based on the previous reports of various groups is shown in Table I. It is obvious that $0.02Ba(Sn_{0.06}Ti_{0.94})O_3$–$0.98(Na_{0.5}K_{0.5})NbO_3$ ceramics have higher k_t/k_p ratios than those reported by various groups.

4. Conclusions

The $0.98(Na_{0.5}K_{0.5})NbO_3$–$0.02Ba(Sn_xTi_{1-x})$ solid solution ceramics were prepared by conventional ceramic sintering. From the XRD patterns, orthorhombic symmetry of 0.98NKN–0.02BST ceramics at room temperature was observed. In piezoelectric ceramics, depending on the crystalline phase, the dielectric constant may be increased or decreased through poling. In this system, the dielectric constant before polarization is larger than that after polarization in the orthorhombic phase. The highest planar coupling factor ($k_p = 0.31$) of $0.98(Na_{0.5}K_{0.5})NbO_3$–$0.02Ba(Sn_xTi_{1-x})O_3$ ceramics is found at $x = 0.02$. For

© 2009 The Japan Society of Applied Physics

$0.02Ba(Sn_{0.06}Ti_{0.94})O_3$–$0.98(Na_{0.5}K_{0.5})NbO_3$ ceramics, the electromechanical coupling coefficients of the planar mode k_p and the thickness mode k_t reach 0.18 and 0.46, respectively, after sintering at 1100 °C for 3 h. The ratio of the thickness coupling coefficient to the planar coupling coefficient is 2.56.

The effects of sintering time on the properties of $0.02Ba(Sn_{0.06}Ti_{0.94})O_3$–$0.98(Na_{0.5}K_{0.5})NbO_3$ ceramics were discussed. The dielectric and piezoelectric properties have better values for 5 h of sintering at 1100 °C. For $0.98(Na_{0.5}K_{0.5})NbO_3$–$0.02Ba(Sn_{0.06}Ti_{0.94})O_3$ ceramics, the electromechanical coupling coefficients of the planar mode k_p and the thickness mode k_t reach 0.24 and 0.49, respectively, after sintering at 1100 °C for 5 h. The ratio of the thickness coupling coefficient to the planar coupling coefficient is 2.02. Prolonged sintering time results in an excessive NKN loss, and the resultant variation in composition leads to an inhomogeneous and loose microstructure. Our results show that $0.02Ba(Sn_{0.06}Ti_{0.94})O_3$–$0.98(Na_{0.5}K_{0.5})NbO_3$ solid solution ceramics are promising lead-free ceramics for high-frequency electromechanical transducer applications.

Acknowledgement

The authors acknowledge the financial support of the National Science Council (under contract NSC-96-2215-E-232-002) of the Republic of China.

1) G. Shirane, R. Newnham, and R. Pepinsky: Phys. Rev. **96** (1954) 581.
2) M. D. Maeder, D. Damjanovic, and N. Setter: J. Electroceram. **13** (2004) 385.
3) V. Lingwal, B. S. Semwal, and N. S. Panwar: Bull. Mater. Sci. **26** (2003) 619.
4) H. Birol, D. Damjanovic, and N. Setter: J. Eur. Ceram. Soc. **26** (2006) 861.
5) T. Takenaka, H. Nagata, and Y. Hiruma: Jpn. J. Appl. Phys. **47** (2008) 3787.
6) S.-Y. Chu, W. Water, Y.-D. Juang, J.-T. Liaw, and S. B. Dai: Ferroelectrics **297** (2003) 11.
7) M. Matsubara, T. Yamaguchi, K. Kikuta, and S. Hirano: Jpn. J. Appl. Phys. **44** (2005) 6136.
8) S. H. Park, C. W. Ahn, S. Nahm, and J. S. Song: Jpn. J. Appl. Phys. **43** (2004) L1072.
9) Y. Guo, K. Kakimoto, and H. Ohsato: Jpn. J. Appl. Phys. **43** (2004) 6662.
10) Y. Guo, K. Kakimoto, and H. Ohsato: Appl. Phys. Lett. **85** (2004) 4121.
11) Y. Guo, K. Kakimoto, and H. Ohsato: Mater. Lett. **59** (2005) 241.
12) M. Kosec, V. Bobnar, M. Hrovat, J. Bernard, B. Malic, and J. Holc: J. Mater. Res. **19** (2004) 1849.
13) Y. Guo, K. Kakimoto, and H. Ohsato: Solid State Commun. **129** (2004) 279.
14) R. C. Chang, S. Y. Chu, Y. F. Lin, C. S. Hong, and Y. P. Wong: J. Eur. Ceram. Soc. **27** (2007) 4453.
15) R. C. Chang, S. Y. Chu, Y. F. Lin, C. S. Hong, P. C. Kao, and C. H. Lu: Sens. Actuators A **138** (2007) 355.
16) V. Cieminski, J. Langhammer, H. T. Abicht, and H. P. Peculiar: Phys. Status Solidi A **120** (1990) 285.
17) V. Mueller, A. Kouvatov, R. Steinhausen, H. Beige, and H.-P. Abicht: Integrated Ferroelectr. **63** (2004) 81.
18) T. Senda and R. C. Bradt: J. Am. Ceram. Soc. **73** (1990) 106.
19) K. Okazaki and K. Nagata: J. Am. Ceram. Soc. **56** (1973) 82.
20) K. H. Hardtl: Ferroelectrics **12** (1976) 9.
21) V. A. Isupov and Yu. E. Stolypin: Sov. Phys. Solid State **12** (1970) 2067.
22) E. G. Fesenko, A. Y. Dantsiger, L. A. Resnitohenko, and M. F. Kupriyanov: Ferroelectrics **41** (1982) 137.

 © 2009 The Japan Society of Applied Physics